Static Force Characteristic and Thermal Field for a Plunger-Type AC Electromagnet

Ioan C. Popa*, Alin-Iulian Dolan†, Constantin Florin Ocoleanu†

* University of Craiova, Department of Electrical Engineering, Craiova, Romania, ipopa@elth.ucv.ro
† University of Craiova, Department of Electrical Engineering, Craiova, Romania, adolan@elth.ucv.ro

Abstract - **In this paper we propose an approach for the determination of static force characteristic of a plunger-type AC electromagnet using 2D numerical model developed in QuickField software and the determination of the thermal field. The attraction electromagnetic force is calculated using Maxwell stress tensor method. The magnetic numerical model is an AC magnetics problem coupled with the coil electric circuit. The magnetic numerical model has been experimentally validated. The thermal field is determined in steady-state regime. The source term in the thermal model equation is calculated from the magnetic model data.**

Cuvinte cheie: modelare numerică, electromagnet de tip plonjor, caracteristica statică a forței de atracție, forța electromagnetică, câmpul termic

Keywords: numerical modeling, plunger type electromagnet, static force characteristic, electromagnetic force, thermal field

I. INTRODUCTION

The plunger-type electromagnets are mainly used in construction of AC low voltage equipments as shutter for minimum voltage [1]. This type of electromagnet is characterized by a large displacement of the plunger. Our goal in this study is to determine the attraction static force characteristic of a plunger-type AC electromagnet by numerical modeling. This is very useful in the analyses of dynamic behavior, the 2D numerical models being quick and easy tools [2]-[5]. On the other hand, this study aims to highlight the error that occurs when using a 2D numerical model. To this purpose, the numerical model should be verified by experimental determinations.

The contribution of the frontal parts of the linkage inductance is negligible on the 2D numerical model, being difficult to calculate. The ohmic resistance of the frontal parts can be taken into account by including an additional resistance in the circuit model which can be easily calculated. However, the numerical results should be validated by analytical methods or experiments.

II. ELECTROMAGNET GEOMETRY

In the paper two models of geometry of a plunger type AC electromagnet were analyzed (model 1 and model 2) with dimensions presented below.

The model 1 (Fig. 1) uses the dimensions: H = 78.6 mm, L = 114.3 mm, b = 32.4 mm, T = 66.2 mm, h_p = 64 mm, c = 22 mm, l = 15.5 mm, t_1 = 11.25 mm, g_m = 12.3 mm, g_j = 13.5 mm, d = 1.8 mm, e = 2.5 mm, δ_2 = 6.9 mm, δ_1 = 1.9 mm, h_b = 41.6 mm. The model 2 uses: H = 110 mm, L = 110 mm, b = 25 mm, T = 64 mm, h_p = 95 mm, c = 22 mm, l = 14 mm, t_1 = 42 mm, g_m = 15 mm, g_j = 15

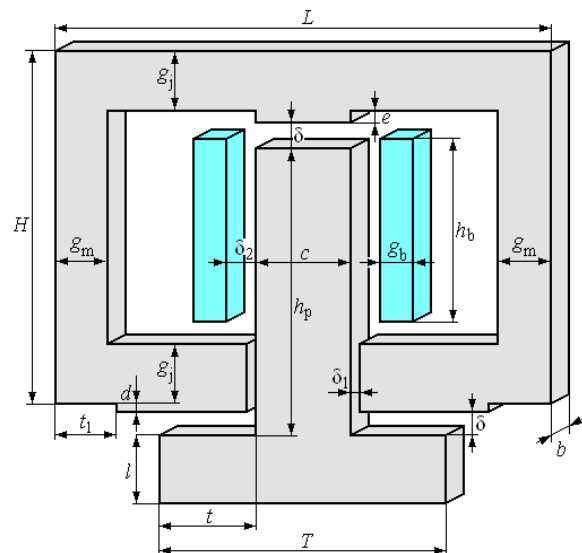mm, d = 0 mm, e = 0 mm, δ_2 = 2 mm, δ_1 = 2 mm, h_b = 77 mm.

Fig. 1. Geometry of the plunger-type AC electromagnet (Number of turns: N = 1250, conductor diameter of the coil: d_c = 0.55 mm, winding resistance R_b = 13.59 ohms).

III. 2D NUMERICAL MODEL

The numerical model is an AC magnetics problem coupled with the coil electric circuit.

A. Magnetic model equation

The fundamental equation of the magnetic field [6], [7] using finite elements method, written in terms of the magnetic vector potential is

$$\frac{\partial}{\partial x}\left(\frac{1}{\mu}\frac{\partial A}{\partial x}\right) + \frac{\partial}{\partial y}\left(\frac{1}{\mu}\frac{\partial A}{\partial y}\right) - j\omega\sigma A = -J_0 \qquad (1)$$

where A is the magnetic vector potential which has only z-direction component, μ is the permeability (in numerical model the relative permeability is μ_r = 1000), σ is the electric conductivity and J_0 is the current source density which is parallel to magnetic vector potential.

B. Thermal model equation

In steady-state regime the thermal governing equation is

$$\frac{\partial}{\partial x}\left(\lambda \frac{\partial T}{\partial x}\right) + \frac{\partial}{\partial y}\left(\lambda \frac{\partial T}{\partial y}\right) + S = 0 \qquad (2)$$

where T is the temperature, λ is the thermal conductivity and S is the source term (power losses in winding, core and plunger).

The source term S contains two components: electromagnet coil losses and magnetic core losses. Knowing the volume occupied by the coil, the specific losses in the coil are calculated based on the total Joule loss $R_b I^2$, where R_b is the total resistance of the coil including its front parts.

The specific losses (W/m³) in the magnetic core are calculated using the Bertotti relationship [7]

$$P = P_{hyst} + P_{eddy} + P_{excess} \qquad (3)$$

where

$$P_{hyst} = k_h f B_m^2 \qquad \text{hysteresis loss}$$

$$P_{eddy} = k_c f^2 B_m^2 \qquad \text{eddy current loss}$$

$$P_{excess} = k_e (f B_m)^{3/2} \qquad \text{excess loss}$$

The coefficients k_h, k_c and k_e depend on the type of magnetic core (supplied by the manufacturer). In the calculations the used values were: k_h = 202, k_c = 0.116, k_e = 3.31. Magnetic flux density (pick value) is an average value provided by the magnetic model for core and plunger. In the thermal model, the ambient temperature was considered to be 20 °C. The calculated specific losses based on the magnetic model and required in the thermal model are shown in Table I.

TABLE I.
CALCULATED LOSS FOR THERMAL MODEL

Material	Loss [W/m³]
Winding	23390
Core	8853
Plunger	10311

C. Electric circuit model coupled to field problem in QuickField software

The electric circuit created in QuickField is shown in Fig. 3 and it contains the source voltage U, the coil ("winding+" and "winding-"), the additional series resistance R_{bf} which denotes the frontal resistance of the coil neglected by the field model and R_a is the variable additional resistance to control the static force characteristic (Fig. 9).

D. Maxwell force

Time average and oscillating component of Maxwell force [2], [7], [8], [9], [10], [11] acting on armature is

$$\vec{F} = \frac{1}{2}\oint_S \left(\vec{H}(\vec{n}\cdot\vec{B}) + \vec{B}(\vec{n}\cdot\vec{H}) - \vec{n}(\vec{H}\cdot\vec{B})\right) dS \qquad (4)$$

where the integral is evaluated over the boundary of the volume defined by surface S enclosing the armature core and $\vec{n}$ denotes the vector of the outward unit normal.

E. Boundary conditions

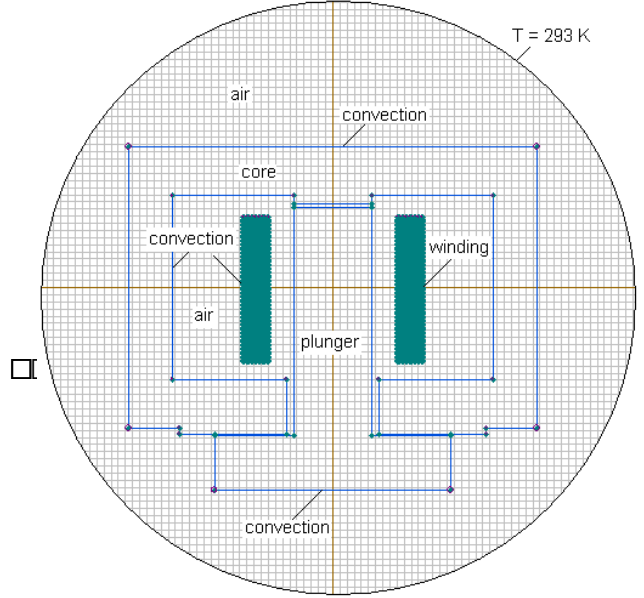For the magnetic model the boundary condition

Fig. 2. Boundary conditions for thermal model.

(which is a circle located at a distance of about 10 times the largest dimension of the modeled object) is a potential magnetic vector with zero value (A = 0).

For the thermal model the boundary conditions are illustrated in Fig. 2.

IV. EXPERIMENTAL METHOD

The experimental determination of the static characteristic of the electromagnet was achieved by the method of detachment of the mobile armature: the voltage is reduced until the armature detaches, when the voltage and current are measured. Taking into account that in linear range of *B-H* curve the force is proportional to the square of the voltage and the current is proportional to the voltage, the force and the current for the rated voltage of the coil are calculated.

Thus, for a certain air gap, after the plunger has been attracted, the voltage is reduced until it breaks out. At the time of detachment, the U_d voltage and the I_d current are measured and the electromagnetic force is counterbalanced by the gravitational force $G = m \cdot g$ of the plunger together with the spacers (made of insulating material) that create the air gap. Finally, their weight is determined.

The force at the rated voltage, for an air gap k is determined by the relationship

$$F_k = mg\left(\frac{U_n}{U_{dk}}\right)^2 \qquad (5)$$

and the current I_{nk} for the same air gap k and voltage is calculate with the relationship

$$I_{nk} = I_{dk}\frac{U_n}{U_{dk}} \qquad (6)$$

where m is the mass of plunger with the spacers, g is the gravitational acceleration, U_{dk} and I_{dk} are the voltage and the current to detachment for the air gap k.
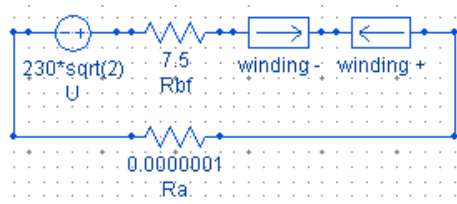

Fig. 3. Electric circuit model coupled to field model in QuickField.

V.   RESULTS AND DISCUSSIONS

Figure 4 shows the current in winding at zero air gap. Figure 5 shows the spectrum of magnetic flux density lines for a particular air gap. In Fig. 6 are shown the numerical and experimental static force characteristics. The numerical results are obtained by numerical model of the electromagnet with geometry shown in Fig. 1 (model 1). It is noted that for a critical range of air gap between 12 and 14 mm the numerical force characteristic presents a minimum. For experimental static force characteristic the critical range of air gap is between 8 and 12 mm.

In Fig. 7 is presented the variation of the current (RMS value) versus air gap at rated voltage ($U_n = 230$ V). It is found that the experimental value of the current is smaller than the numerical value, because in this case the current limitation is also affected by the frontal linkage reactance of the coil. The difference between the experimental and the numerical values increases with the increase of the air gap.

Figure 8 shows the variation of the inductance versus the air gap obtained by the numerical model and by the experimental method. In this case the differences are very small.

Figure 9 shows the variation of the linkage flux versus the air gap.

Figure 10 shows the variation of the impedance versus air gap which has similar form as that of Fig.8.

Figure 11 shows the static characteristic of the attraction force for model 2 of electromagnet.

If the ratio H / L is greater or equal the unit (model 2 of geometry), the minimum of the static characteristic is more pronounced (Fig. 9). This minimum can be attenuated or even eliminated with an additional resistance in series with the winding.
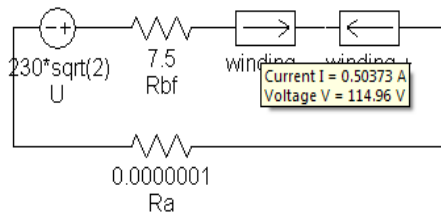

Fig. 4. Current in electric circuit model at zero air gap.

In Fig. 12 shows the thermal field of device and in Fig. 13 shows the temperature variation along line AB.

The heat transfer coefficient on the core and plunger surfaces was considered to have a value of 8 $Wm^{-2}K^{-1}$ and of 7 $Wm^{-2}K^{-1}$ on the coil surface.
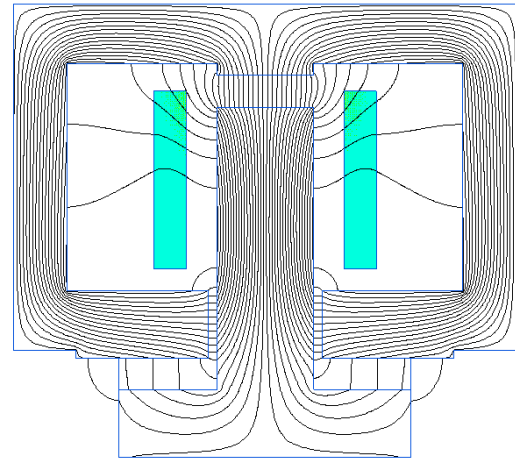
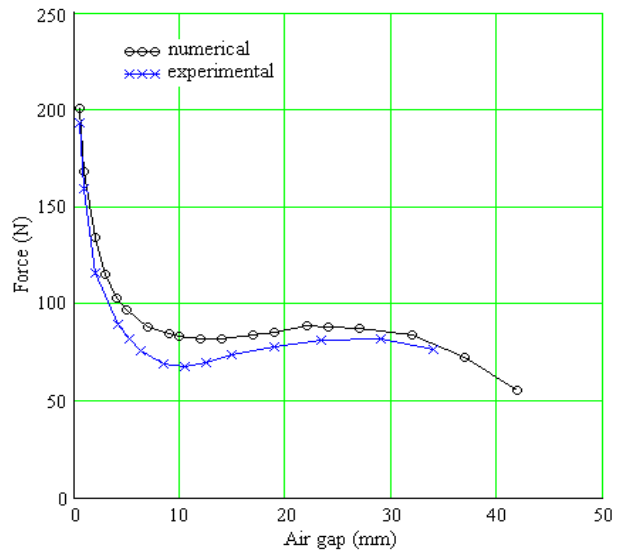

Fig. 5. Magnetic flux density lines.

Fig. 6. Static force characteristic without additional resistance (model 1).
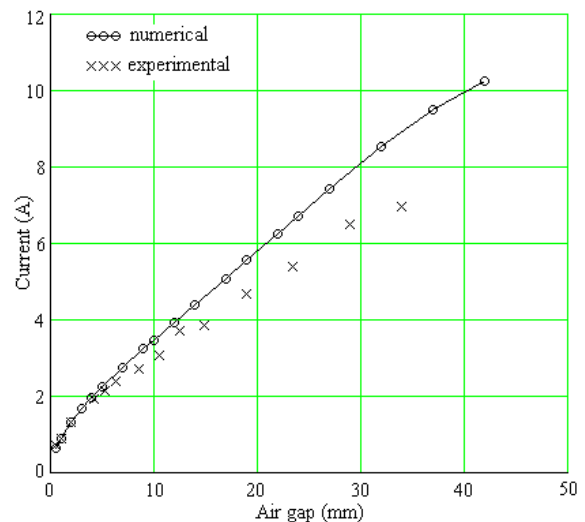

Fig. 7. The current versus air gap without additional resistance.

If the ratio H/L is greater or equal the unit (model 2 of geometry), the minimum of the static characteristic is more pronounced (Fig. 11). This minimum can be attenuated or even eliminated with an additional resistance in series with the electromagnet coil (the characteristics $k = 4$ and $k = 8$). If the minimum is pronounced, after a short voltage interruption, the armature can no longer be attracted, remaining "hanging" at the critical air gap. Under these conditions, the coil will be thermally overstressed.

Figure 4 shows that the 2D numerical model is acceptable for determining the static force characteristic. The maximum error related to experiment is about 22.65%. This error is linked to the range of critical air gap.

Figure 5 shows that the experimental value of the current is lower and it increases with the air gap. This is explained by the fact that the numerical model does not consider the reactance of the frontal parts of the coil.
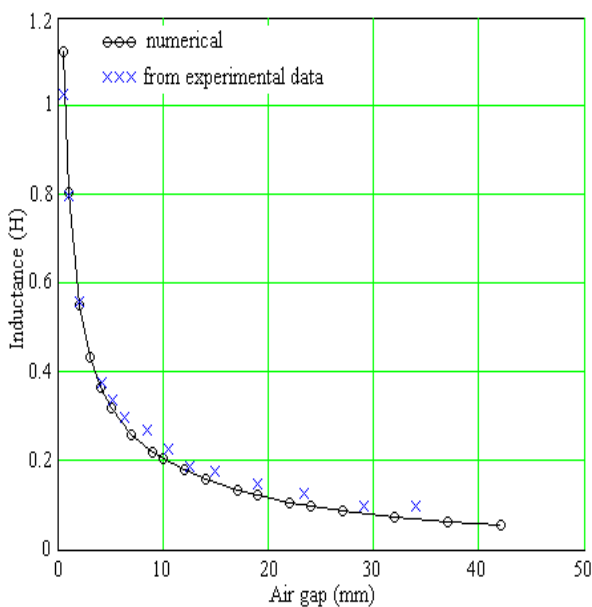

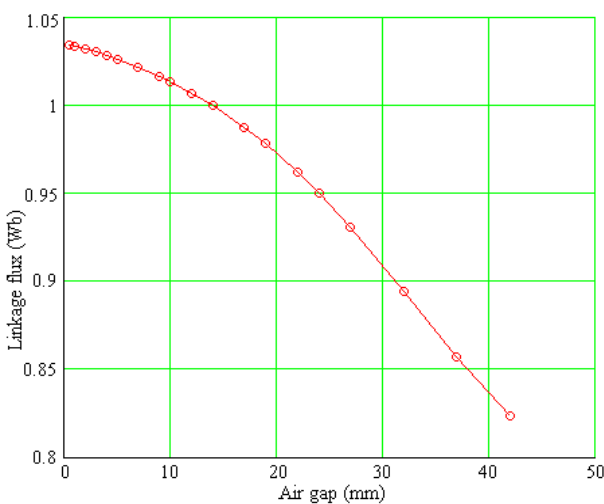Fig. 8. Electromagnet linkage inductance versus air gap.

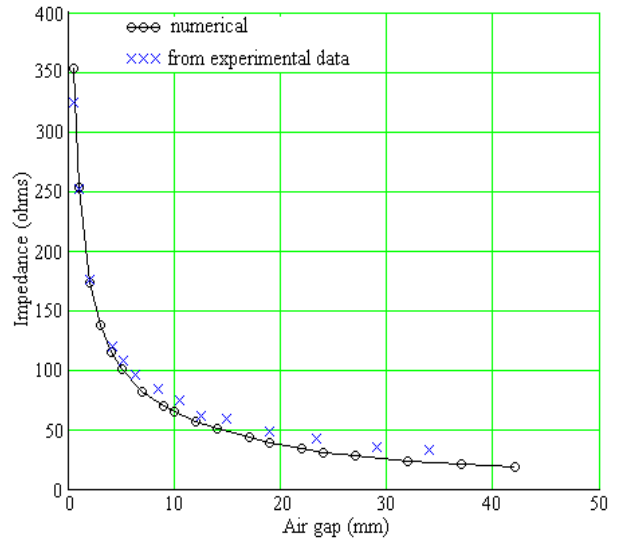Fig. 9. Linkage flux versus air gap (numerical).
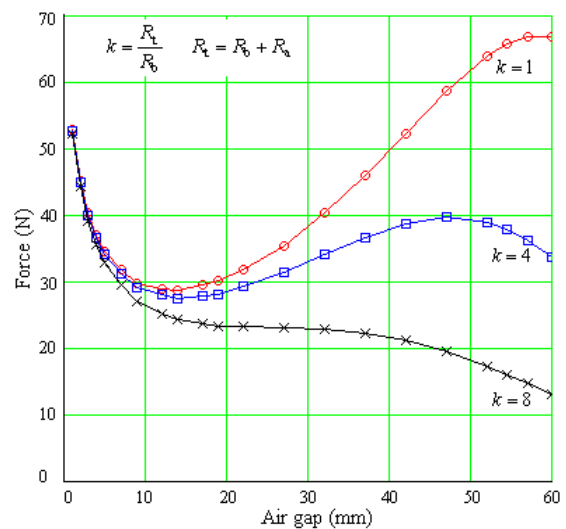

Fig. 10. Electromagnet impedance versus air gap.

Fig. 11. Static force characteristic for different additional resistance ($k = 1$: numerical, without additional resistance) (model 2).
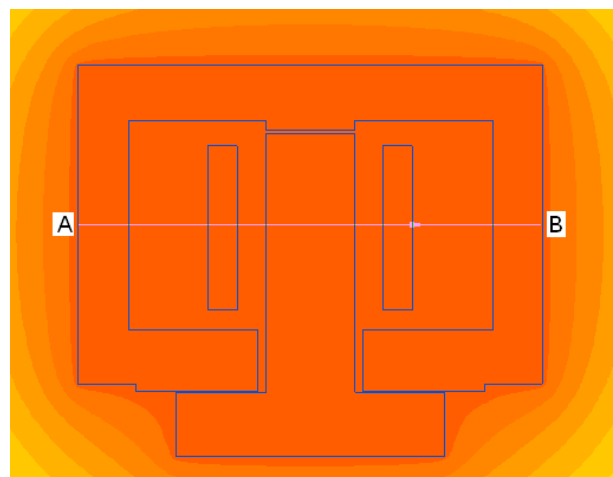

Fig. 12. Distribution of thermal field ($k = 1$: numerical, without additional resistance) (model 2).
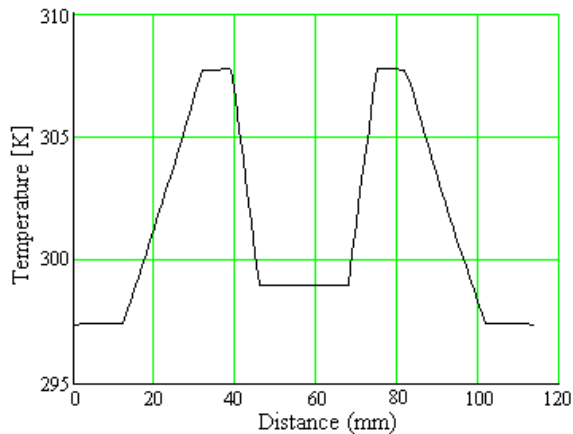
Fig. 13. Temperature variation along line AB (from Fig. 12).

VI.   CONCLUSIONS

The developed 2D numerical models experimentally validated can be used to estimate the attraction force characteristic and thermal field of plunger-type AC electromagnets within the limits of the presented error.

This model can be used to optimize the static force characteristic and of electromagnet design.

Although in the electric circuit coupled with the field problem the contribution of the front part of the ohmic resistance of the coil (measured or calculated) is introduced, this is insignificant because of its value much lower than the reactance at air gaps less than 10 mm. At higher air gaps, the reactance becomes comparable to resistance.

A 3D numerical model is certainly more accurate but the computing time to obtaining the static characteristic is much higher.

ACKNOWLEDGMENT

Contribution of authors:
First author – 80%
First coauthor – 15%
Second coauthor – 5%

REFERENCES

[1]   G. A. Cividjian, I. Popa, M. Leoveanu, "Attraction force of electromagnets with armature in T," National Conference on Electrical and Power Engineering, Vol. 9 Electrical Apparatus, Timişoara, September 1982, pp. 65-70.

[2]   Y. Kawase, and S. Ito, "Analysis of attactive force of pull-type single phase a.c. electromagnets," IEEE Trans. Magn., vol. 26, No. 2, pp. 1046-1049, March 1990.

[3]   Y. Kawase, O. Miyatani, T. Yamaguchi, and S. Ito, "Numerical analysis of dynamic characteristics of electromagnets using 3D finite element method with edge elements," IEEE Trans. Magn., vol. 30, pp. 3248-3251, September, 1994.

[4]   Y. Kawase, O. Miyatani, K. Iawashita, T. Kobayashi, and K. Suzuki, "3-D Finite element analysis of dynamic characteristics of electromagnet with permanent-magnets," IEEE Trans. Magn., vol. 42, pp. 1339-1342, April, 2006.

[5]   M. Bartsch, and T. Weiland, "2D and 3D Calculation of forces," IEEE Trans. Magn., vol. 30, pp. 3467-3470, September, 1994.

[6]   I. Popa, A-I. Dolan, "Static Force Characteristic of E-Type Single Phase AC Electromagnets," International Conference on Applied and Theoretical Electricity (ICATE 2014), Craiova, 2014, pp. 1-5.

[7]   *** http://www.quickfield.com, QuickField, Finite Element Analysis System, Version 6.3, User's Guide.

[8]   M. Jufer, "Circuits magnétiques – Exemples et applications, Techniques de l'ingénieur," Edition TI, réf. 1051, Février 2007.

[9]   F. Leplus, "Bobine à noyau de fer en régime variable," Techniques de l'ingénieur, Edition TI, réf. D-3010, Février 2007.

[10] P. L. Kalantarov and L. A. Teitlin, "Inductances Calculation," (in roumanian), Editura Tehnică, Bucureşti, 1958.

[11] Ziwei Ouyang, Juan Zhang and William Gerard Hurley, "Calculation of Leakage Inductance for High Frequency Transformers," IEEE Transactions on Power Electronics, vol. 30, No. 10 October 2014, pp. 5779 – 5775.